A Comprehensive Experimental, Numerical, Economic, and Environmental Evaluation of an Innovative Solar Still Design for the Desalination of Najaf Seawater

Yasir Fayez Youssif [1], Mohammed Alfahham [2*], and Hassanain Ghani Hameed [3]

[1,2,3] Al-Furat Al-Awsat Technical University, Engineering Technical College/Najaf, Najaf, Iraq

muntadher.saeed2@yahoo.com, coj.moh@atu.edu.iq, hassanain.hameed@atu.edu.iq

Abstract

Solar stills are generally characterized by their low production cost and ease of installation and operation. Its low productivity is the deciding factor in its limited widespread use. In this study, a monoclinic solar still with a polygonal absorber plate and an arc-shaped back side(PASS) was fabricated and tested. The new design makes the most of the curved back side by installing a wall reflector, which maximizes the concentrated solar radiation on the base. We compared the performance of the presented model (PASS) with the conventional one (CSS). Both models are made from the same raw materials and have the same absorbent plate area. To ensure the accuracy of the results, a specially designed numerical program was developed using COMSOL Multiphysics V6.3. The results showed a close agreement between the numerical model and the experimental results. In practice, the new enhanced design increased yield by approximately 175.3% compared to the conventional model, resulting in a 68.21% reduction in the cost of producing one liter and a 265.43% reduction in carbon emissions treatment costs.

Index-words: Advanced Solar still design, Najaf Sea, Fresh water production, Renewable desalination technology, PCM, energy-water nexus.

Nomenclature		Subscripts	
A	area (m²)	a	ambient
CSS	Conventional solar still	b	basin
cp	specific heat (J/kg K)	c	convection
h	heat transfer coefficient (W/m² K)	d	daily
Hf	Front height of still (m)	s	Sky
Hr	Rear height of still (m)	e	evaporation
I	solar radiation intensity (W/m²)	g	glass
k	thermal conductivity (W/m K)	r	radiation
m	mass (kg)	ins	insulation
P	productivity (kg/m²)	w	water layer
PASS	polygonal solar still	**Greek**	
T	temperature (C°)	τ	transmissivity
t	time (sec)	ρ	density (kg/m³)
U	heat loss coefficient (W/m² K)	σ	Stefan-Boltzmann's constant (W/m²K⁴)
X	thickness (m)	ε	emissivity
h_{fg}	Water latent heat of vaporization $(\frac{J}{Kg})$	η	efficiency (%)
T_{sun}	Sun temperature	Θ	angle of inclination (Degree)

I.   Introduction

Water scarcity has become one of humanity's most critical global challenges due to human and urban growth [1]. With the turmoil in energy market prices, the increase in demand, and the associated climate challenges, all of this has reinforced the trend towards using environmentally friendly energy. Wilson tested the first real solar distillation device in 1883 [2]. Later, researchers studied many designs to develop the solar stills [3-8]. Velmurugan et al. [9] experimentally increased the yield by 75% when they used a corrugated absorption plate and a layer of waste rubber, sand, and marble mixture. The study by Hadj et al. [10] had a yield enhancement of about 105% due to their use of wall-mounted trays filled with sand and an internal reflector. The use of the double-slope design resulted in an increase in yield by about 57.83% [11]. Davra et al. [12] were able to practically increase overall efficiency by 86.57% using a stepped design enhanced with a layer of raw paraffin. A conventional solar still combined with a passive condenser can enhance yields by 30% to 150% [13]. Adding nanoparticles to the absorption surface of a conventional distiller resulted in an increase in the output value by 17.06% [14]. Abdullah et al. [15] used an internal copper heating tube to increase the total production of the conventional still by about 76%. Saha et al. [16] presented an experimental study that included using a double-slope vacuum design and pure paraffin as a heat storage material, which increased the output by about 63% compared to the conventional design. Z. Xu et al. [17] designed and tested a multi-stage solar still with an output boost of about 75%. Many studies have been presented, including the extent to which the operation of the solar distiller is affected in terms of production and efficiency by the surrounding environmental climatic conditions [18, 19]. Devagar and Mohanraj [20] presented an economic analysis that estimated the expected lifespan of a solar still operating at full efficiency for ten years. Through environmental analysis, the study showed that using solar distillation reduced pollution by approximately 14.1 tons and saved $338.4 in energy. The best productivity can be achieved at a raw water depth of 1–2 cm [21]. Several studies have been presented that list the most important factors affecting the efficiency and performance of solar stills [22-24].

Various studies presented by many researchers have noted that the geometric shapes used are conventional, double, cylindrical, spherical, conical, and others.

In this research paper, a unique design of a single-slope solar still is proposed through an experimental study of a polygonal base solar still with an arc side and a comparison of the results obtained with a conventional still under the climatic conditions of the Najaf Sea region, Iraq.

Compared to previous literature, the large inner wall of the model is utilized through a curved design and is configured to support the vertical reflector mounted on it. This enables the use of multiple improvers, resulting in a 175.3% yield improvement compared to conventional trailers (CSS).

II.   Experimental setup

The test model was designed to consist of an 8 cm thick cork container containing a uniquely shaped absorbent base, as shown in Figure 1. A 4 mm thick glass cover is placed at a 32.1-degree angle on top of the cork box. Figure 2 shows a schematic of the device in use with its accessories. Inside the cork container, we placed a 1 mm thick 0.25 absorber plate and a matte black galvanized iron plate. The saline level inside the basin was adjusted to 1 cm using a small cylindrical mechanical float.

In accordance with the latitude of Najaf, Iraq, and at a tilt angle of 32.1 degrees, the upper tilted glass cover layer is securely attached using transparent heat adhesive.

Through a 4 cm diameter plastic channel fixed under the lower end of the glass cover, the condensed water drops are collected and delivered to a graduated collection flask placed at the balance level.

Three different instruments were calibrated and used to measure the temperatures of the various system components and the atmospheric conditions of the experiment. The first instrument was a Hit-HT-9815 electronic thermometer, which reads temperatures via an array of connected thermocouples. A Metravi-207 was used to measure solar radiation intensity, while a PCE-420 was used to estimate wind speed.
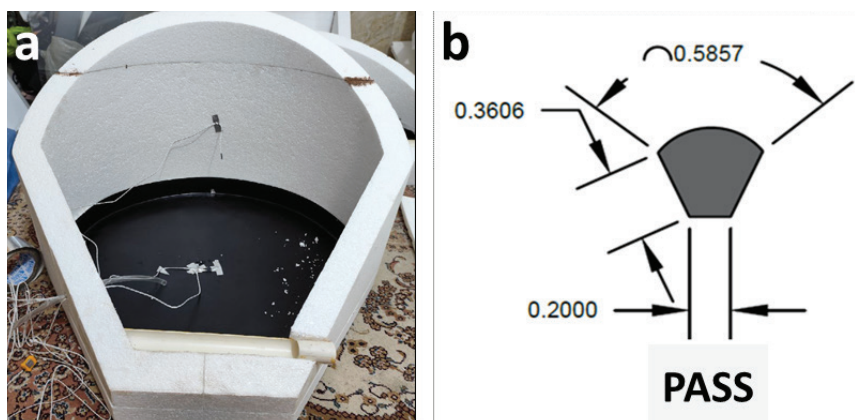
Figure 1: (a) and (b), Actual dimensions, base shape, and frame design of the model presented in this study.
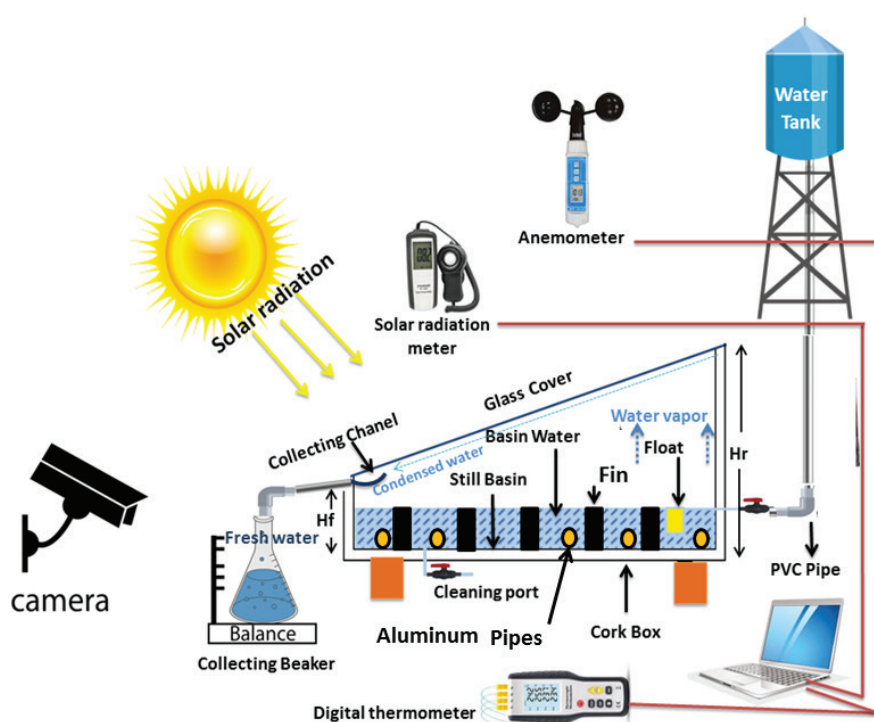

Figure 2: Schematic diagram of the practical experiment.

A.   Vertical wall reflector specifications

As shown in Figure 3, using inexpensive, highly reflective aluminum foil attached to the curved vertical wall of the cork structure from the inside, the internal reflector allows for greater solar radiation concentration onto the black absorber surface. Increasing the radiation concentration on the absorber plate raises its Temperature, which raises the Temperature of the turbid water layer it contains, causing a rapid increase in the amount of steam produced and, consequently, a higher yield of fresh water.

Figure 3: Solar still with internal reflector.

B.   Aluminum pipes filled with Najaf sea sand

A set of one-centimeter-diameter aluminum tubes was extracted from the scrap yard at Najaf Technical College, filled with gray sand from the Najaf sea, and tightly sealed at both ends. The tubes were completely coated with a matte black varnish, and the five tubes were placed inside the turbid water tank, as shown in Figure 4. Because the opaque tubes have good thermal storage capacity, they help heat the water longer after sunset, increasing the yield.

C.   Aluminum tubes filled with Iraqi paraffin wax mixed with graphite powder

As shown in Figure 4, from scrap metal, we used five 1cm diameter black aluminum pipes after filling them with Iraqi paraffin wax mixed with graphite powder extracted from the remains of graphite pens and car brake linings. The graphite was combined with the wax at a ratio of 10%. Table 1 shows the physical properties of the paraffin wax blend versus the graphite-wax mixture. Graphite increases the thermal conductivity of the paraffin wax, increasing the mixture's ability to absorb and deliver heat, reducing heat loss, and making the system more sensitive to energy. The presence of this mixture works to exploit thermal energy for the longest possible time after sunset. It enhances the evaporation and production processes, increasing the system's efficiency.

Figure 4: Polygonal solar still enhanced with black-filled heat storage tubes.

Table 1: Physical properties of paraffin wax blend versus graphite -wax mixture [6, 25]

Specification	Paraffin wax	Graphite	graphite -wax mixture
Density (kg/m³)	ρ_{solid} = 880 ρ_{liquid} = 770	2100	1002
Specific heat (Cp) (J/kgK)	2000	765	1876
Thermal conductivity (W/mK)	k = 0.2	0.75	0.26
Viscosity (μ) (Ns/m²)	$0.001 exp(-4.25+1790/T)$	------	0.0778
Latent heat (L) (J/kg)	160	-----	144
Melting Temperature (oC)	56	-----	56

D.   Use of hollow hexagonal fins

As shown in Figure 5, twenty-five nuts are seamlessly welded to the absorber plate. These nuts are 2 cm in diameter and 1 cm thick, have a 1.2 cm hollow core, and are fully coated with black thermal varnish. These fins increase the contact area between the absorber plate and the turbid water layer, which contributes to transferring a greater amount of heat to the turbid water layer, thereby reducing heat evaporation time and increasing the water yield.

Figure 5: Polygonal solar still enhanced with hexagonal fins.

E. Use of a layer of Limestone

As shown in Figure 6, Limestone extracted from the Najaf Seawater shelf is characterized by its physical and chemical stability. It has good conductivity, does not dissolve or decompose easily in water, and does not alter the appearance or taste of water. Moreover, it is widely available. We used a layer of Limestone approximately 1 cm thick to cover the black absorption plate. The stone effectively absorbs heat during the day and releases it at night. It also increases the contact area with the brine layer, which stimulates the heating and evaporation of the solution, increasing the yield.

Figure 6: Polygonal model reinforced with Limestone.

F. Using a layer of burnt date pits inside the turbid water basin

Using a 0.5 kg layer of burnt date pits, a 0.8 cm thick layer is formed inside the brine layer of the solar still, as shown in Figure 7. This addition enhances the thermal storage capacity of solar radiation due to its dark color. The porosity between the pits significantly increases the absorption surface area, which positively impacts the evaporation rate of seawater and, consequently, increases the production yield.

Figure 7: The polygon solar still that uses a layer of burnt date pits.

G. Use of Thassos stone

The addition of Thassos stone within the expanded collector channel enhanced the creation of a thermal gradient within the system, as shown in Figure 8. The stone has a cool porous structure, which facilitates greater and faster steam condensation and prevents steam accumulation within the enclosed area, thus enhancing production and preventing steam retention.

Figure 8: The model is equipped with an enlarged collection channel filled with Thassos stone.

III.   Steps related to the application aspect

From a raised plastic tank, seawater flows through transparent, flexible tubes with a diameter of 0.5 cm into the solar still's absorber plate. A mechanical cylindrical float adjusts the seawater level inside the still to 1 cm.

As the incoming solar radiation reaches the absorber plate through the transparent cover and raw water layers, as shown in Figure 9, the Temperature of the absorber plate begins to rise over time due to the increasing amount of solar radiation. Crucially, conduction transfers heat from the absorbent black plate to the seawater layer. This causes the water layer to gradually warm up, leading to increased evaporation over time. Due to the temperature difference between the glass and the vapor at the inner surface of the inclined glass cover, the vapor condenses in the form of a film that slides toward the lower end of the glass cover. The water droplets sliding off the glass cover collect in a 2 cm diameter plastic channel securely attached at the slanted lower end of the cover. Due to the channel's slanted attachment, the water droplets slide out to collect in a balanced graduated glass flask.

Figure 10 shows the local ambient climate conditions of the Najaf Sea region on April 18, 2025 (the day and location of the experiment). The experiment lasted from 8 a.m. to 10 p.m., with hourly measurements of various temperature variables, production values, and meteorological parameters (solar radiation intensity, local wind speed, and air temperature). Figure 11 and Table 2 show a site-specific listing of the measuring equipment used in the practical experiment. The presence of a plastic control valve under the absorption plate serves as a continuous cleaning operation to remove accumulated dirt from the use of Najaf seawater.

Under the same conditions and specifications, the performance of the proposed model (PASS) was compared with that of the conventional model with a square-based, the same area of the black absorber plate, as shown in Figure 12.
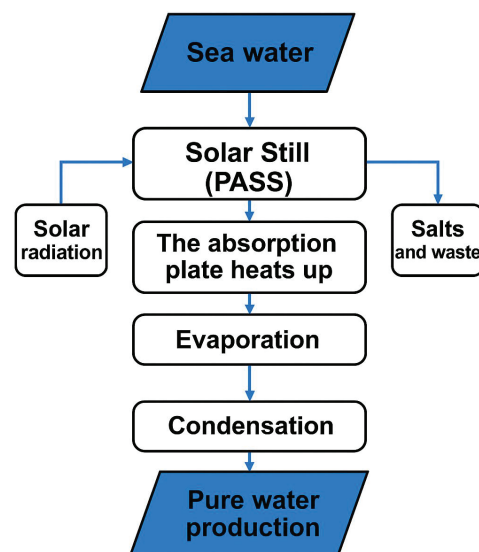

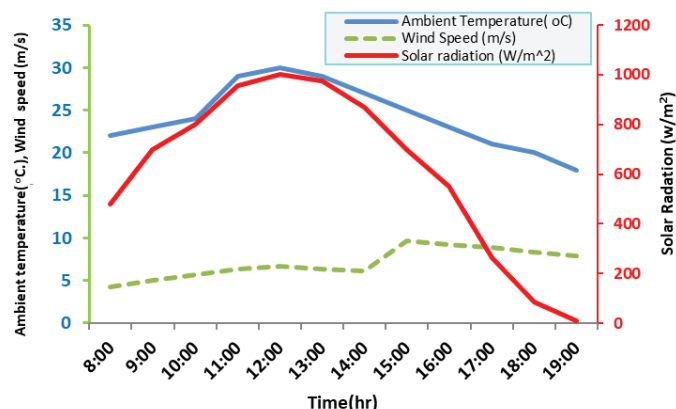Figure 9: A flowchart of the solar still system is presented in this study.

Figure 10: The climatic conditions surrounding the Najaf Sea area during the practical testing of the model on 18/4/2025.
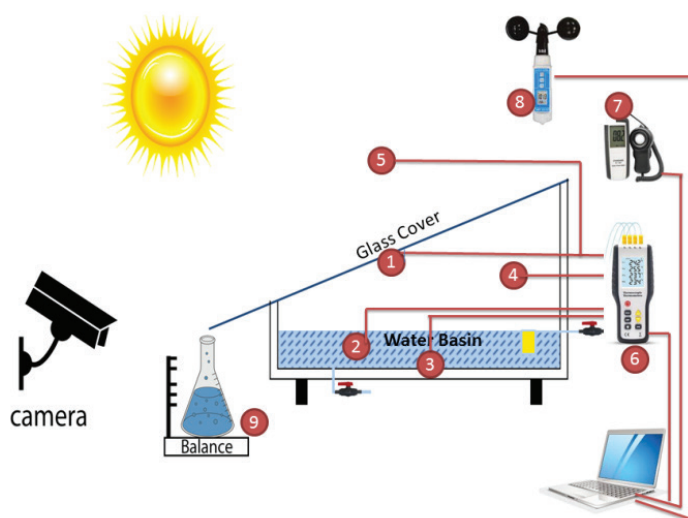

Figure 11: Mounting points of various measuring equipment used in the practical aspect.

Table 2: Mounting points of various measuring equipment used in the practical aspect

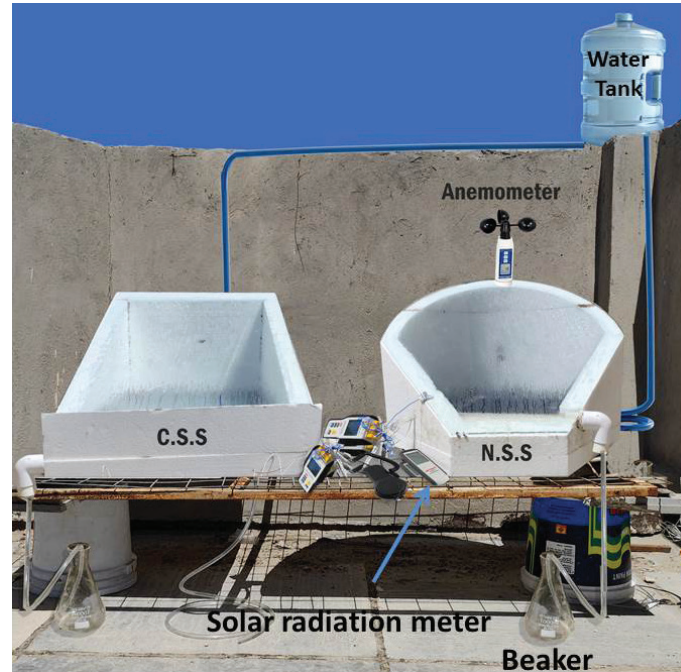| Measuring tool	Thermocouples	Digital thermometer	Solar radiation sensor	Anemometer	Water collection bottle
Action point	1-5	6	7	8	9

Figure 12: Real models are used in practical experiments.

IV. Mathematical analysis of the model

Using COMSOL Multiphysics V6.3, a three-dimensional numerical analysis was performed to predict the temperature values of the absorber plate, seawater layer, transparent cover, and pure water yield values in each hour, as shown in Figure 13.

A. Energy Analysis

1. Assumptions used to facilitate numerical solution [26-29]

- No steam mass leaks out of the system at all.

- The flow within the system is only a laminar flow.

- All variables are related to temperature change.

2. Heat balance equations

The energy of an absorber plate represents the algebraic resultant of the energy gained from solar radiation minus the energy transferred to the water and collateral losses [29, 30].

$$m_b c_{p,b}\left(\frac{dT_b}{dt}\right) = A_w[I\alpha_b - h_{cwb}(T_b - T_w) - U_b(T_b - T_a)] \quad (1)$$

The Temperature of the seawater layer represents the algebraic sum of the heat gained from the absorbing layer and the energy gained from solar radiation, which is less than the amount of heat lost (convection, radiation, and evaporation) to the glass cover.

$$m_w c_{p,w}\left(\frac{dT_w}{dt}\right) = A_w[I\alpha_w + h_{cbw}(T_b - T_w)] - A_w h_{wg}(T_w - T_g) - A_w U_{ins,w}(T_w - T_a) \quad (2)$$

The heat gained by the cover from the seawater (convection, radiation, and evaporation) is equal to the heat lost by the cover outside the system.

$$m_g c_{p,g}\left(\frac{dT_g}{dt}\right) = A_g \alpha_g I + A_w h_{wg}(T_w - T_g) - A_g h_{rgs}(T_g - T_s) - A_g h_{cga}(T_g - T_a) \quad (3)$$

By applying boundary conditioning, initial parameters, and the effect of the real climatic parameters of the study area on day 18-5, the previous equations were solved to obtain the hourly production value [31].

$$P_d = \frac{dm_e}{dt} = h_{wg} \frac{[T_w - T_g]}{[h_{fg}]}$$ (4)

$$h_{fg} = 2.4935 \times 10^6 \times (1 - 9.478 \times 10^{-4} T_w + 1.3132 \times 10^{-7} T_w^2 - 4.7974 \times 10^{-9} T_w^3)$$ (5)

While the thermal efficiency of the new device (PASS) can be calculated as:

$$\eta_{daily} = \frac{\sum (P_d \, h_{fg})}{3600 \, A \sum I_t}$$ (6)

Table 3 displays the real specifications and characteristics of the model that the program uses.

Table 3: Specifications of the model parts required by the numerical program

Parameter	Value	Parameter	Value	Parameter	Value
ε_g	0.88	k_{ins} (w/m.k)	0.03	$x_b(m)$	0.001
τ_g	0.9	cp_w (J/kg K)	4190	ρ_b (kg/m³)	7870
τ_w	0.95	A_w (m²)	0.25	$\sigma(W/m^2 \, K^4)$	5.669x10⁻⁸
α_b	0.9	$x_g(m)$	0.004	m_w (kg)	2.5
α_g	0.05	Cp b (J/kg K)	460	Θ (Degree)	32.1
α_w	0.05	k_b (W/m.K)	73	$U_{ins}(\frac{w}{m^2 k})$	0.5
ε_w	0.96				
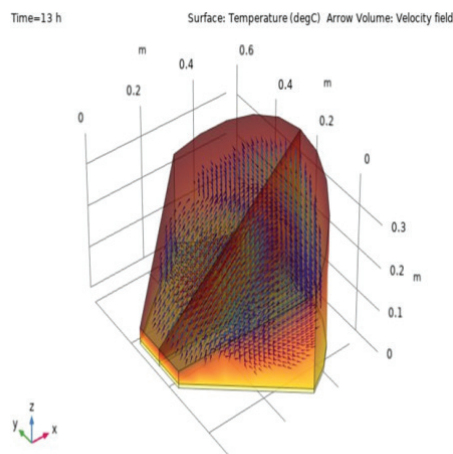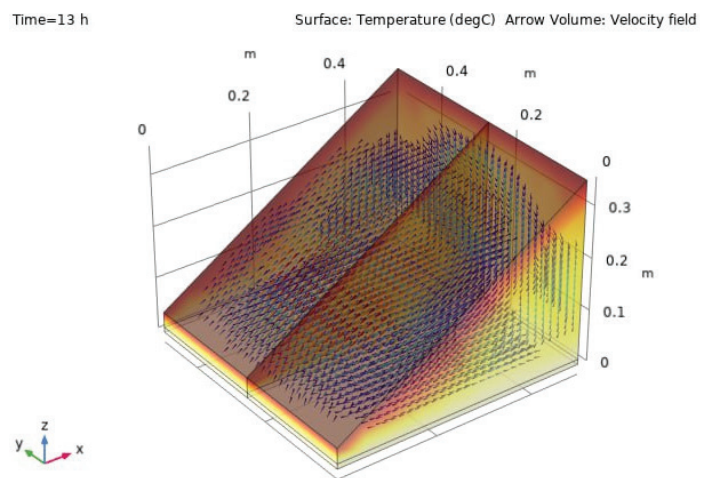
Figure 13. The numerical models prepared through this study.

PASS

CSS

3.   Initial and boundary conditions

To optimize the program and obtain the most accurate results, the simulation must begin with realistic and specific initial and boundary conditions.

1.   The initial seawater temperature was set at 20°C, which is consistent with the ambient Temperature for the study day.

2.   The initial atmospheric pressure was set at 101.325 kPa as the initial limit for the simulation.

3.   At (t > 0), the no-slip condition is applied to ensure realistic thermal equilibrium.

4.   To ensure outstanding and realistic results, the accompanying weather conditions and how they interact with the external boundaries of the model are considered.

3	Solar meter	$\pm 1.2\frac{w}{m^2}$	0-3000 $\frac{w}{m^2}$	0.2
4	Anemometer	$\pm 0.11\frac{m}{s}$	0-25 $\frac{m}{s}$	9.9
5	Flask	$\pm 10\ ml$	0-1000	10

V. Comparison of the physical, chemical, and biological specifications between the water produced from the distillation device and the water of the Najaf Sea

A physical, chemical, and biological analysis of the available surface water in the Najaf Sea was carried out and compared with the same specifications of the yield water produced by the device with the innovative design. Table 4 shows an actual comparison of this water.

Table 4: Specifications of water from the solar still compared to Najaf seawater

Parameters		Najaf Sea	Distilled water
PH		30	7.3
TDS (mg/l)		37500	45
Negative Ions (PPM)	HCO_3	18000	57
	CI	84977	6
	SO_4	4081	4
Positive Ions (PPM)	K	805	1
	Na	1045	6
	Mg	11344	2
	Ca	1763	6
Escherichia coli		widespread	Not found

From Table No. 4, we note that the water produced from the solar distillery has specifications that make it suitable for human consumption.

VI. Uncertainties assessment

The error percentage for the various measuring equipment used in the practical aspect was calculated based on the general equation for determining uncertainty [31, 32], as shown in Table 5.

$$\partial f = \sqrt{\left(\frac{\partial f}{\partial x_1}\delta x_1\right)^2 + \left(\frac{\partial f}{\partial x_2}\delta x_2\right)^2 + \cdots + \left(\frac{\partial f}{\partial x_n}\delta x_n\right)^2} \quad (7)$$

Table 5: Calculating the accuracy, range, and error of measuring equipment (thermocouples, temperature reading device, digital solar radiation reading device, wind speed measuring turbine, and yield collecting flask)

No.	Equipment	Accuracy	Range	%Error
1	Thermocouples	± 0.98 ℃	0-200 ℃	0.125
2	Thermometer	± 3℃	-100-1300 ℃	0.45

VII. Discussion of the results achieved

Table 6 shows a real comparison of the experimental products, including the maximum and minimum temperatures of the water and glass layers and the percentage of yield enhancement for the polygonal model without and with improvements such as the use of (wall reflector, aluminum tubes filled with Najaf sea and/ or Iraqi paraffin wax, hexagonal fins, Limestone, and burnt date pits).

All tested models were compared with a conventional model manufactured with the same specifications, materials, and absorption panel area.

Adding various enhancers to the (PASS) model has also increased yields by varying amounts. The outputs achieved listed that the maximum yield improvement value was about 11.7, 23.48, 137.66, 35.1, 71.43, 57.15, 16.9, and 175.3% for (PASS, PASS-PS, PASS-IR, PASS-HF, PASS-L, PASS-PG, PASS-DP, and PASS-RLT), respectively, as compared to the reference model.

The results showed that using a polygonal solar still with an internal reflector, Limestone, and a larger collection channel filled with Thassos marble (PASS-RLT) produced about 175.3% more water than a regular solar still (CSS). This is due to the use of a vertical reflector, which increases the concentration of solar radiation toward the absorber base, raising its Temperature. The use of Limestone also accelerates the absorption and evaporation processes due to its porous structure and high capacity for heat absorption. Meanwhile, the Thassos stone laid in the collection channel increases the condensation process due to its unique physical composition, which gives it a cooler property. The use of these improvers has significantly increased the overall yield.

Figure 14 shows a comparison of the enhancement ratios achieved in the current study with the enhancement ratios of several different previous designs compared to a conventional solar still.

Table 6: Min. and max. Limits for temperatures and production enhancement values achieved through practical experiments.

| No.	Model type	During high radiation (1002 w/m²)				During low radiation (260 w/m²)			
		T_w (°C)	T_g (°C)	Yield (ml)	%Increase in Yield	T_w (°C)	T_g (°C)	Yield (ml)	%Increase in Yield
1	Conventional still (CSS)	59.2	43.1	77	Ref.	40.3	33.4	37	----
2	Polygonal Solar still (PASS)	67.8	44.4	86	11.7	42.7	33.6	42	13.52
3	Polygonal Solar still with Aluminum pipes filled with Najaf sea sand (PASS-PS)	72.1	44.7	95	23.4	46.5	34.2	46	24.35
4	Polygonal Solar still with internal reflector (PASS-IR)	92.3	45.8	183	137.66	50.8	34.4	67	81.1
5	Polygonal Solar still with hexagonal fins (PASS-HF)	74.8	44.2	104	35.1	46.4	34.5	44	19
6	Polygonal Solar still with Limestone (PASS-L)	81.7	45.0	132	71.43	47.4	35.2	60	62.2
7	Polygonal Solar still with paraffin wax and graphite powder (PASS-PG)	76.2	44.1	121	57.15	49.9	35.2	65	75.7
8	Polygonal Solar still with date pits (PASS-DP)	68.9	44.7	90	16.9	54.1	33.7	45	21.62
9	Polygonal Solar still with internal reflector, Limestone, and expanded collection channel filled with Thassos marble (PASS-RLT)	94.3	45.8	212	175.3	61	34.5	78	111
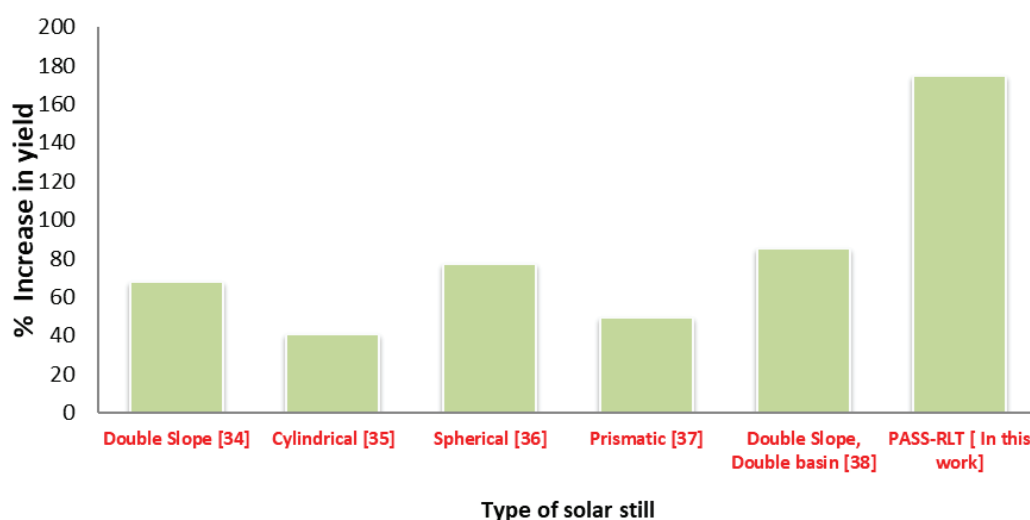
Figure 14: Production enhancement ratios of the model presented in this study, along with a group of models offered in previous studies, are compared to a conventional solar still [34-38].

Figure 14 demonstrates the significant superiority of the improved polygonal solar still, which achieved a 175.3% increase in yield compared to the reference model, making it superior to many designs presented by previous researchers.

A.   Effect of changing the tilt angle of the vertical reflector on the amount of output achieved

Under the climatic conditions of the Najaf Sea region, on 18/4/2025, a practical test was conducted to determine the extent of the effect of the vertical reflector tilt angle on the amount of fresh water production.

The reflector was tilted at angles (0, 4, 8, and 12) degrees relative to the column. The experiments, conducted under the same weather conditions for all models, found that the best output was 1529 ml/day when the vertical reflector was tilted at an angle of 8 degrees, as shown in Figure 15.
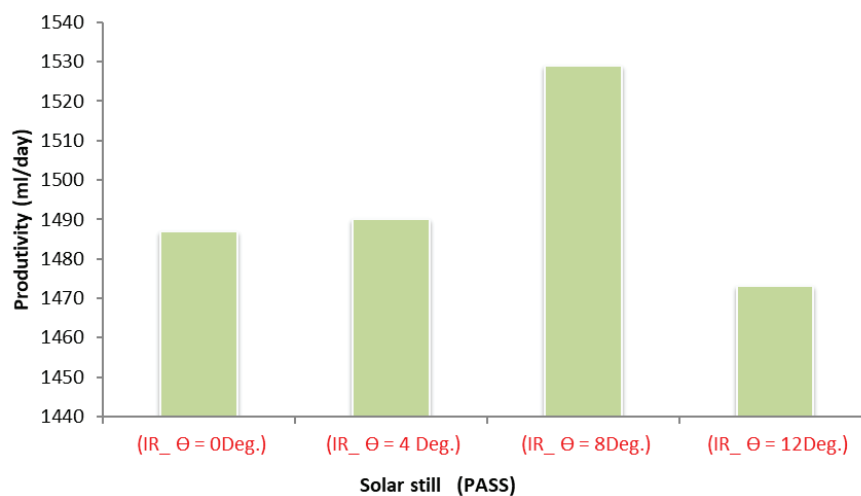

Figure 15: The effect of the tilt angle of the wall reflector from the column on the production of the tested solar still (PASS).

B.   Comparison between the results obtained practically and the numerical results

By looking at the real experimental results and comparing them to the numerical model created with the COMSOL V6.3 software, which was made for this specific task and under the same weather conditions as the real experiment, the simulation results matched very well, with an error rate of no more than 6%.

Figure 16 illustrates the comparison between the actual output and the results from the numerical simulation program, which was executed under the same atmospheric conditions as those for the practical experiment listed in Figure 10.
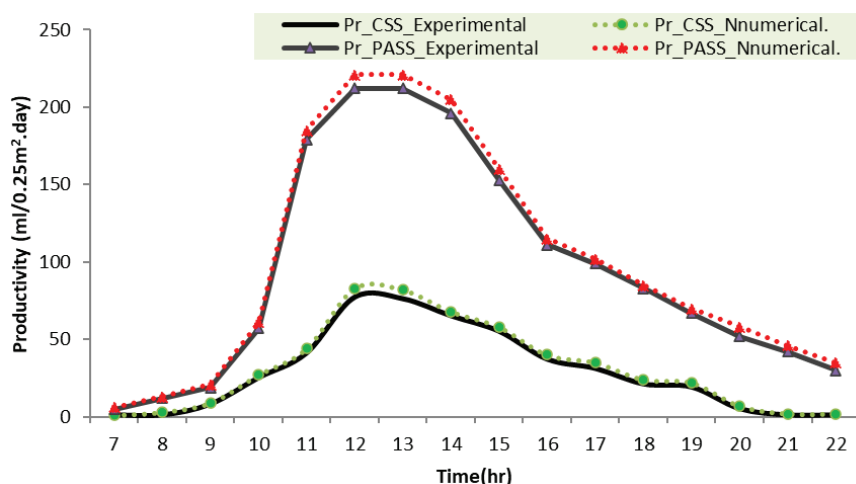

Figure 16: Comparison of the practical and numerical productivity of the polygonal solar still (PASS) and the reference conventional solar still (CSS).

VIII. Economic analysis of polygonal Still (PASS)

Using the approved equations [39 and 40], the costs are analyzed (C), and the economic viability of the polygonal solar still is shown compared to the conventional still, as shown below:

$$C = Fixed\ Cost(F) + Variable\ Cost(V) \qquad (8)$$

$$V = 10 \times 0.2 \times F \qquad (9)$$

Using Table 7, the manufacturing cost of the practically tested models (PASS and CSS) was calculated.

$$C_{PASS} = 21 + (10 \times 0.2 \times 21) = 63\$$$

$$C_{CSS} = 20 + (10 \times 0.2 \times 20) = 60\$.$$

The total daily freshwater yield is 1529 ml per 0.25 m² for the polygonal model and 464 ml per 0.25 m² for the conventional model.

Since the device's expected lifespan is 10 years and the number of days the device is operating is 300 days/year, the total expected yield during the device's expected lifespan can be 4587 liters/m² and 1392 liters/m² for the polygonal (PASS) and conventional (CSS) models, respectively.

More simply, the cost of producing one liter of fresh water can be predicted as follows:

For the conventional model (CSS): $\frac{C_{CSS}}{1392} = \frac{60}{1392} = 0.0431$ \$ for one liter only.

And, for polygonal (PASS): $\frac{C_{SES}}{4587} = \frac{63}{4587} = 0.0137$ \$ for one liter only.

Table 7: Costs of materials used to form parts of models used in the practical experiment

No.	Type of part	Specifications	Cost ($)	
			PASS	CSS
1	Structure	0.11m³	6.5	6.5
2	4mm thick transparent cover	0.35m²	3	2.5
3	Basin plate	0.26m²	7	7
4	Strips of aluminum foil	0.5m²	0.5	—
5	Black dye	1 piece.	1	1
6	Silicone adhesive	1 piece.	1	1
7	Plastic pipes	3 pieces.	2	2
	Total Cost		21	20

IX. Environmental analysis

Based on data from the Iraqi Ministry of Environment, the average carbon dioxide emissions per unit of energy are estimated at 0.99 kg/kWh. Using solar desalination reduces carbon dioxide emissions by approximately 16.25 tons over the still's estimated 10-year lifetime [40].

With energy losses during transmission and distribution approaching 40% and household appliance losses at around 20%, this simultaneously raises CO_2 emissions to 1.58 kg/kWh [40].

A.   Embodied energy

It is the energy consumed to produce or form a particular part.

Table 8 shows the embodied energy(E_{in}) for all parts of the working model [40].

Table 8: The embodied energy (E_{in}) for all parts of the working model [40]

No.	Material type	Mass (Kg)	Energy density (kWh/kg)	E_{in} (kWh)	
				PASS	CSS
1	Cork structure	0.8 kg	2.8	2.24	2.24
2	4mm thick transparent cover	3.3 kg	5.2	17.16	17.16
3	0.1 mm thick galvanized iron sheet	1.4	12.4	17.36	17.36
4	Dark opaque paint	0.2	3.2	0.64	0.64
5	Thermal silicone glue	0.25	3.4	0.85	0.85
6	PVC fittings	0.75	20.1	15	15
	Total			53.25	53.25

B. CO_2 emission

Using the equation below, the amount of carbon dioxide emissions (ψ_{CO_2}) can be predicted over the lifetime of the presented model [40].

$$\psi_{CO_2} = \frac{Embodied\ energy(E_{in}) \times 1.58}{Still\ life} \qquad (10)$$

C.   Reducing carbon dioxide emissions

A measure of a country's ability to cope with climate change, and denoted as $Ʒ_{CO_2}$ [40]

$$Ʒ_{CO_2} = \frac{[(E_{out} \times n) - E_{in}]1.58}{1000} \qquad (11)$$

And, Annual energy production $(E_{out}) = \frac{yearly\ yield \times h_{fg}}{3.6 \times 10^6}$ (kWh)

D. Carbon credit earned (CCE)

The concentration of carbon dioxide in the air in a given geographic area is one of the most important indicators of the amount of emissions to combat climate change.

It can be calculated as follows [40-42]:

$$CCE = \mathfrak{z}_{co_2} \times Average\ cost\ gained\ from\ processing\ per\ ton\ of\ carbon\ (D)$$ (12)

D = 20$/ton of Co_2 mitigation, and 1$=1430ID (Dated 25/6/2025).

Based on the presented set of equations, Table 9 lists the energy analysis and carbon pccroperty values of the solar stills presented in this study.

Table 9: Energy analysis of the stills

No.	Model	Yearly output(kg)	E_{in} (kWh)	E_{out} (kWh)	ψ_{co_2} (kg/year)	$\mathfrak{z}_{co_2}$	CCE (ID)
1	PASS	458.7	53.25	296.82	8.414	4.606	131731.6
2	CSS	139.2	53.25	85.1	8.414	1.260	36048.73

As a result of this modern design (PASS), the cost of eliminating carbon waste was reduced by an estimated 265.43% compared to the reference model (CSS).

X.   Conclusion

Under the real climatic conditions of the Najaf Sea area, Najaf city, central Iraq, an experimental and numerical study of a monoclinic solar still with an innovative polygonal design was conducted. To improve the production process, several useful changes were made, including using a vertical wall reflector, hollow hexagonal fins, Limestone, Iraqi paraffin wax mixed with graphite powder, Najaf sea sand, and burnt date pits.

Consequently, compared the obtained results with the conventional model and came to the following conclusions:

1.   The new solar distillation unit makes greater use of available solar radiation through a concave inner wall design, allowing for the installation of an internal reflector.

2.   To achieve maximum productivity, a vertical internal reflector is installed next to the curved wall at an 8-degree angle, further concentrating radiation toward the black base.

3.   Aluminum tubes filled with paraffin wax mixed with graphite powder or filled with Najaf sea sand were used as heat storage materials inside the raw water basin.

4.   The raw Najaf seawater supplies the entire system. As is well known, the productivity of a distiller operating with highly turbid and polluted seawater is lower than that of less turbid and less saline water.

5.   It was also shown that the intensity of solar radiation is directly proportional to the value of the achieved production, as the value of the practically achieved production approaches the value of the theoretical results obtained by computer.

6.   Practical experience showed that the daily output achieved by the polygonal still was 1529ml/0.25m^2, while the conventional still achieved a daily output of 464 ml/0.25m^2 Thus, the polygonal model achieved an increase in daily production of about 229.53% compared to the conventional one.

7.   The use of 0.25 kilograms of paraffin wax enhanced with graphite powder, packed in tightly closed tubes and immersed in a basin of water, had an effect on enhancing production by 57.15%.

8.   The new design offers a significant reduction in the cost of producing eachliter of fresh water by approximately 68.21% compared to the conventional model.

9. As a result of this modern design (PASS), the cost of eliminating carbon waste was reduced by an estimated 265.43% compared to the reference model (CSS).

10. The new design provides broad possibilities for future experiments for researchers to develop the model and test more parameters that would increase the production quantity, such as using more methods for cooling the glass cover, such as mechanical vibrations or cooling using compressed gases, or testing larger sizes of external solar reflectors, etc.

Availability of data and material

I understand that the journal may be available in print and online, and will be made available to a wider audience through marketing channels and other third parties. Therefore, anyone can read the material published in it. I recognize that the readership may include not only engineers and academic researchers, but also journalists and the general public.

We, the authors, declare that there is no conflict of interest with any party.

References

[1] P. Dumka and D. R. Mishra, "Experimental investigation of modified single slope solar still integrated with earth (I) &(II):Energy and exergy analysis," *Energy*, vol. 160, pp. 1144–1157, Oct. 2018, doi: 10.1016/j.energy.2018.07.083.

[2] R. M. Wilson, "Yellowstone and the Making of a New West Western," *Montana*, vol. 74, no. 1, pp. 61–76, Mar. 2024, doi: 10.1353/mnt.2024.a922409.

[3] M. El Hadi Attia, A. E. Kabeel, N. A. Moharram, W. M. El-Maghlany, and M. Fayed, "Enhancing freshwater yield in conical solar stills utilizing external reflective mirrors: An experimental approach," *Solar Energy*, vol. 288, p. 113287, Mar. 2025, doi: 10.1016/j.solener.2025.113287.

[4] A. Elsheikh *et al.*, "Integrating predictive and hybrid Machine Learning approaches for optimizing solar still performance: A comprehensive review," *Solar Energy*, vol. 295, p. 113536, Jul. 2025, doi: 10.1016/j.solener.2025.113536.

[5] G. Singh, P. K. Singh, A. Saxena, N. Kumar, and D. B. Singh, "Investigation of conical passive solar still by incorporating energy metrics, efficiency, and sensitivity analyses for sustainable solar distillation," *J Clean Prod*, vol. 434, p. 139949, Jan. 2024, doi: 10.1016/j.jclepro.2023.139949.

[6] M. M. Ali Saeed, D. M. Hachim, and H. G. Hameed, "Numerical investigation for single slope solar still performance with optimal amount of Nano-PCM," *Journal of Advanced Research in Fluid Mechanics and Thermal Sciences*, vol. 63, no. 2, 2019.

[7] V. Singh, R. Kumar, A. Saxena, R. Dobriyal, S. Tiwari, and D. B. Singh, "An analytical study on the effect of different photovoltaic technologies on enviro-economic parameter and energy metrics of active solar desalting unit," *Energy*, vol. 294, p. 130851, May 2024, doi: 10.1016/j.energy.2024.130851.

[8] S. Nazari and R. Daghigh, "Techno-enviro-exergo-economic and water hygiene assessment of non-cover box solar still employing parabolic dish concentrator and thermoelectric peltier effect," *Process Safety and Environmental Protection*, vol. 162, pp. 566–582, Jun. 2022, doi: 10.1016/j.psep.2022.04.006.

[9] V. Velmurugan, C. K. Deenadayalan, H. Vinod, and K. Srithar, "Desalination of effluent using fin type solar still," *Energy*, vol. 33, no. 11, pp. 1719–1727, Nov. 2008, doi: 10.1016/j.energy.2008.07.001.

[10] L. Hadj-Taieb, A. S. Abdullah, M. Aljaghtham, A. Alkhudhiri, Z. M. Omara, and F. A. Essa, "Improving the performance of trays solar still by using sand beds and reflectors," *Alexandria Engineering Journal*, vol. 71, pp. 659–668, May 2023, doi: 10.1016/j.aej.2023.03.084.

[11]   S. Joe Patrick Gnanaraj, S. Ramachandran, and David Santosh Christopher, "Enhancing the design to optimize the performance of double basin solar still," *Desalination*, vol. 411, pp. 112–123, Jun. 2017, doi: 10.1016/j.desal.2017.02.011.

[12]   D. Davra, P. Mehta, N. Patel, and B. Markam, "Solar-enhanced freshwater generation in arid coastal environments: A double basin stepped solar still with vertical wick assistance study in northern Gujarat," *Solar Energy*, vol. 268, p. 112297, Jan. 2024, doi: 10.1016/j.solener.2023.112297.

[13]   H. Amiri, "Enhancing the stepped solar still performance using a built-in passive condenser," *Solar Energy*, vol. 248, pp. 88–102, Dec. 2022, doi: 10.1016/j.solener.2022.11.006.

[14]   R. Sahu and A. C. Tiwari, "Performance enhancement of single slope solar still using nanofluids at different water depth," *Desalination Water Treat*, vol. 317, p. 100046, Jan. 2024, doi: 10.1016/j.dwt.2024.100046.

[15]   A. S. Abdullah, W. H. Alawee, S. A. Mohammed, A. Majdi, Z. M. Omara, and M. M. Younes, "Utilizing a single slope solar still with copper heating coil, external condenser, phase change material, along with internal and external reflectors — Experimental study," *J Energy Storage*, vol. 63, p. 106899, Jul. 2023, doi: 10.1016/j.est.2023.106899.

[16]   S. Saha, M. R. I. Sarker, M. A. Kader, M. M. Ahmed, S. S. Tuly, and N. N. Mustafi, "Development of a vacuum double-slope solar still for enhanced freshwater productivity," *Solar Energy*, vol. 270, p. 112385, Mar. 2024, doi: 10.1016/j.solener.2024.112385.

[17]   Z. Xu *et al.*, "Ultrahigh-efficiency desalination *via* a thermally-localized multistage solar still," *Energy Environ Sci*, vol. 13, no. 3, pp. 830–839, 2020, doi: 10.1039/C9EE04122B.

[18]   S. K. Singh, S. C. Kaushik, V. V. Tyagi, and S. K. Tyagi, "Comparative Performance and parametric study of solar still: A review," *Sustainable Energy Technologies and Assessments*, vol. 47, p. 101541, Oct. 2021, doi: 10.1016/j.seta.2021.101541.

[19]   M. Muntadher Mohammed Saeed, H. Hameed, and A. Abbass, "Numerical Investigation of the Effect of Wind Speed on Performance of Single-Slope Solar Still," *Solar Energy and Sustainable Development Journal*, vol. 13, no. 2, pp. 174–182, Aug. 2024, doi: 10.51646/jsesd.v13i2.241.

[20]   R. Dhivagar and M. Mohanraj, "Performance improvements of single slope solar still using graphite plate fins and magnets," *Environmental Science and Pollution Research*, vol. 28, no. 16, pp. 20499–20516, Apr. 2021, doi: 10.1007/s11356-020-11737-5.

[21]   S. K. Nougriaya, M. K. Chopra, B. Gupta, P. Baredar, and H. Parmar, "Influence of basin water depth and energy storage materials on productivity of solar still: A review," *Mater Today Proc*, vol. 44, pp. 1589–1603, 2021, doi: 10.1016/j.matpr.2020.11.796.

[22]   S. Nazari, M. Najafzadeh, and R. Daghigh, "Techno-economic estimation of a non-cover box solar still with thermoelectric and antiseptic nanofluid using machine learning models," *Appl Therm Eng*, vol. 212, p. 118584, Jul. 2022, doi: 10.1016/j.applthermaleng.2022.118584.

[23]   S. S. Narayanan, A. Yadav, and M. N. Khaled, "A concise review on performance improvement of solar stills," *SN Appl Sci*, vol. 2, no. 3, p. 511, Mar. 2020, doi: 10.1007/s42452-020-2291-5.

[24]   S. W. Sharshir, N. Yang, G. Peng, and A. E. Kabeel, "Factors affecting solar stills productivity and improvement techniques: A detailed review," *Appl Therm Eng*, vol. 100, pp. 267–284, May 2016, doi: 10.1016/j.applthermaleng.2015.11.041.

[25]   Z. H. Rao and G. Q. Zhang, "Thermal Properties of Paraffin Wax-based Composites Containing Graphite," *Energy Sources, Part A: Recovery, Utilization, and Environmental Effects*, vol. 33, no. 7, pp. 587–593, Jan. 2011, doi: 10.1080/15567030903117679.

[26] K. Selvaraj and A. Natarajan, "Factors influencing the performance and productivity of solar stills - A review," *Desalination*, vol. 435, pp. 181–187, Jun. 2018, doi: 10.1016/j.desal.2017.09.031.

[27] L. D. Jathar *et al.*, "Effect of various factors and diverse approaches to enhance the performance of solar stills: a comprehensive review," *J Therm Anal Calorim*, vol. 147, no. 7, pp. 4491–4522, Apr. 2022, doi: 10.1007/s10973-021-10826-y.

[28] A. Madhlopa, "Theoretical and empirical study of heat and mass transfer inside a basin type solar still," *Energy*, vol. 136, pp. 45–51, Oct. 2017, doi: 10.1016/j.energy.2016.09.126.

[29] H. Diabil, "Performance of A New Model of Air Heating System: Experimental Investigation," pp. 420–432, 2021.

[30] M. M. A. Saeed, H. G. Hameed, and A. A. Abbass, "Design and Testing of a Single-Slope Solar Still With a Semi-Elliptical Absorbent Base: An Experimental and Numerical Study," *Heat Transfer*, vol. 54, no. 4, pp. 2580–2593, Jun. 2025, doi: 10.1002/htj.23258.

[31] H. Hameed, M. M. A. Saeed, H. O. Abdulridha, and D. A. Abdullah, "A Practical Comparative Study of a Single-slope Solar Still with an Enhanced Design," *Renewable Energy & Sustainable Development*, 2024.

[32] N. Rahbar and J. A. Esfahani, "Productivity estimation of a single-slope solar still: Theoretical and numerical analysis," *Energy*, vol. 49, pp. 289–297, Jan. 2013, doi: 10.1016/j.energy.2012.10.023.

[33] Muntadher Mohammed Ali Saeed, Hassanain Ghani Hameed, and Hayder Azeez Neamah Diabil, "Experimental Investigation on Thermal Performance of Solar Air Heater using Nano-PCM," *Journal of Advanced Research in Fluid Mechanics and Thermal Sciences*, vol. 117, no. 1, pp. 83–97, May 2024, doi: 10.37934/arfmts.117.1.8397.

[34] K. Elmaadawy, A. W. Kandeal, A. Khalil, M. R. Elkadeem, B. Liu, and S. W. Sharshir, "Performance improvement of double slope solar still via combinations of low cost materials integrated with glass cooling," *Desalination*, vol. 500, p. 114856, Mar. 2021, doi: 10.1016/j.desal.2020.114856.

[35] M. S. El-Sebaey, A. Ellman, A. Hegazy, and F. A. Essa, "Experimental study with thermal and economical analysis for some modifications on cylindrical sector and double slope, single basin solar still," *Case Studies in Thermal Engineering*, vol. 49, p. 103310, Sep. 2023, doi: 10.1016/j.csite.2023.103310.

[36] A. E. Kabeel, M. El Hadi Attia, M. Abdelgaied, F. A. Essa, and M. F. Aly Aboud, "Comparative performance of spherical, hemispherical, and single-sloped solar distillers," *Desalination Water Treat*, vol. 317, p. 100051, Jan. 2024, doi: 10.1016/j.dwt.2024.100051.

[37] M. E. Zayed *et al.*, "Novel Design of Double Slope Solar Distiller with Prismatic Absorber Basin, Linen Wicks, and Dual Parallel Spraying Nozzles: Experimental Investigation and Energic–Exergic-Economic Analyses," *Water (Basel)*, vol. 15, no. 3, p. 610, Feb. 2023, doi: 10.3390/w15030610.

[38] T. Rajaseenivasan and K. Kalidasa Murugavel, "Theoretical and experimental investigation on double basin double slope solar still," *Desalination*, vol. 319, pp. 25–32, Jun. 2013, doi: 10.1016/j.desal.2013.03.029.

[39] M. Alsehli, "Maximizing solar distillation efficiency and cost-effectiveness with the rotating ball spherical solar still: An energetic, exergetic, and economic analysis," *Process Safety and Environmental Protection*, vol. 182, pp. 234–244, Feb. 2024, doi: 10.1016/j.psep.2023.11.076.

[40] M. M. A. Saeed, H. G. Hameed, and A. Alsahlani, "Numerical Investigation of Single Slope Solar Still Performance With Different Designs: Energy, Exergy, Economic and Environmental Analysis, and Optimization," *Heat Transfer*, vol. 54, no. 6, pp. 4102–4123, Sep. 2025, doi: 10.1002/htj.23402.

[41] V. Kumar, B. Das, and R. Gupta, "Energy, exergy, economic and environmental analyses of single slope solar still employing cylindrical cement fins and wick material for thermal energy storage," *J Energy Storage*, vol. 110, p. 115360, Feb. 2025, doi: 10.1016/j. est.2025.115360.

[42] A. E. Kabeel, M. El Hadi Attia, M. Abdelgaied, F. A. Essa, and M. F. Aly Aboud, "Comparative performance of spherical, hemispherical, and single-sloped solar distillers," *Desalination Water Treat*, vol. 317, p. 100051, Jan. 2024, doi: 10.1016/j.dwt.2024.100051.